



저작자표시-비영리-변경금지 2.0 대한민국

이용자는 아래의 조건을 따르는 경우에 한하여 자유롭게

- 이 저작물을 복제, 배포, 전송, 전시, 공연 및 방송할 수 있습니다.

다음과 같은 조건을 따라야 합니다:



저작자표시. 귀하는 원저작자를 표시하여야 합니다.



비영리. 귀하는 이 저작물을 영리 목적으로 이용할 수 없습니다.



변경금지. 귀하는 이 저작물을 개작, 변형 또는 가공할 수 없습니다.

- 귀하는, 이 저작물의 재이용이나 배포의 경우, 이 저작물에 적용된 이용허락조건을 명확하게 나타내어야 합니다.
- 저작권자로부터 별도의 허가를 받으면 이러한 조건들은 적용되지 않습니다.

저작권법에 따른 이용자의 권리는 위의 내용에 의하여 영향을 받지 않습니다.

이것은 [이용허락규약\(Legal Code\)](#)을 이해하기 쉽게 요약한 것입니다.

[Disclaimer](#)

A Thesis
For the Degree of Master of Veterinary Medicine

The role of progranulin
as a novel therapeutic target
for experimental autoimmune
encephalomyelitis

Department of Veterinary Medicine

GRADUATE SCHOOL

JEJU NATIONAL UNIVERSITY

Jinhee Cho

2016. 2

The role of progranulin as a novel therapeutic target for experimental autoimmune encephalomyelitis

Jinhee Cho

(Supervised by professor Youngheun Jee)

A thesis submitted in partial fulfillment of the requirement
for the degree of Master of Veterinary Medicine

2015. 12.

This thesis has been examined and approved by

Thesis director, Taekyun Shin, Prof. of Veterinary Medicine

Youngheun Jee, Prof. of Veterinary Medicine

Meejung Ahn, Research Prof. of Medicine

Department of Veterinary Medicine
GRADUATE SCHOOL
JEJU NATIONAL UNIVERSITY

CONTENTS

Contents	1
List of tables	2
List of figures	3
List of abbreviations	4
Abstract	6
Introduction	7
Materials and methods	10
Results	17
Discussion	20
References	24
Tables	30
Figures	33
Abstract in Korean	42

LIST OF TABLES

Table 1. Primers sequences for PGRN and GAPDH

Table 2. Immunoreactivity of PGRN on various cells in spinal cords

Table 3. Summary of active clinical parameters

LIST OF FIGURES

- Figure 1.** Disease symptom scores and relative expression of PGRN in EAE mice.
- Figure 2.** PRGN was overexpressed in glial cells and inflammatory cells of the spinal cord during EAE development.
- Figure 3.** PRGN was overexpressed on astrocytes.
- Figure 4.** PRGN was overexpressed on microglia.
- Figure 5.** Double fluorescence staining revealed PGRN-positive CD4⁺ T cells, CD8⁺ T cells, and CD11b⁺ positive macrophages in the spinal cords of EAE mice.
- Figure 6.** Clinical scores of MOG₃₅₋₅₅ induced EAE in WT and PGRN^{-/-} mice.
- Figure 7.** Infiltration of inflammatory cells into lumbar spinal cord sections obtained from WT EAE and PGRN^{-/-} EAE mice.
- Figure 8.** PGRN depletion impaired the proliferation of MOG₃₅₋₅₅ reactive splenic mononuclear cells.

LIST OF ABBREVIATIONS

MS	Multiple sclerosis
EAE	Experimental autoimmune encephalomyelitis
CNS	Central nervous system
PGRN	Progranulin
GRN	Granulin
FTD	Frontotemporal dementia
IBD	Inflammatory bowel disease
DSS	Dextran sodium sulfate
RA	Rheumatoid arthritis
MOG	Myelin oligodendrocyte glycoprotein
PLP	Proteolipid protein
MBP	Myelin basic protein
CFA	Complete Freund's adjuvant
PT	Pertussis toxin
Con A	Concanavalin A
H&E	Hematoxylin and eosin
SE	Standard error
DAB	3,3'-diaminbenzidine tetrachloride
HRP	Horseradish peroxidase
BSA	Bovine serum albumin
GFAP	Glial fibrillary acidic protein

Iba-1	Ionized calcium binding adaptor protein
CD	Cluster of differentiation
STAV	Streptoavidin
FITC	Fluorescein isothiocyanate
TRITC	Tetramethylrhodamine
DAPI	4', 6-diamidino-2-phenylindole dihydrochloride
cDNA	Complementary deoxyribonucleic acid
mRNA	Messenger ribonucleic acid
Real-time PCR	Quantitative real-time polymerase chain reaction
GAPDH	Glyceraldehyde-3-phosphate dehydrogenase
Ct	Cycle threshold
PMSF	Phenylmethylsulfonyl fluoride
SDS-PAGE	Sodium dodecyl sulfated polyacrylamide gel electrophoresis
ECL	Enhanced chemiluminescence reagent
HEPES	4-(2-hydroxyethyl)-1-piperazineethanesulfonic acid
NEAA	Non-essential amino acid
β -ME	Beta-mercaptoethanol
FBS	Fetal bovine serum
P/S	Penicillin-Streptomycin
ANOVA	Analysis of Variance

1. ABSTRACT

Experimental autoimmune encephalomyelitis (EAE) characterized by inflammation and demyelination in central nervous system (CNS) is used as an animal model of human multiple sclerosis (MS) because its symptoms reflects pathophysiologic steps in MS. Progranulin (PGRN) is a secreted glycoprotein which has many roles in diverse biological processes such as inflammation, wound repair, and cellular proliferation. The purpose of this study was to elucidate the role of PGRN expression in the course of EAE. PGRN expression was increased dramatically by astrocyte, microglia and infiltrated inflammatory cells at the disease peak. Furthermore, PGRN^{-/-} mice showed significantly ameliorated paralysis. These results suggest that PGRN might be involved in the mouse EAE, and would be potential therapeutic target for human demyelinated CNS disease.

Key words: Progranulin (PGRN), Experimental autoimmune encephalomyelitis (EAE), Multiple sclerosis (MS)

2. INTRODUCTION

Multiple sclerosis (MS) are an inflammatory and demyelinating autoimmune disease in the central nervous system (CNS) (Baxter. 2007). Experimental autoimmune encephalomyelitis (EAE) is used to test potential therapeutic agents of MS because pathologic and clinical similarities of EAE are similar to that of human MS (Steinman L. 1999). When susceptible strains of mice immunized with components of myelin such as myelin oligodendrocyte glycoprotein (MOG), proteolipid protein (PLP) or myelin basic protein (MBP), EAE is induced by infiltration of myelin-reactive T cells and macrophages, as well as activation of endogenous glial cells (Martin and McFarland. 1995).

Although the inflammatory and neurodegenerative phase of MS is considered largely mediated by auto-reactive T cells and macrophages, neurotransmitters such as glutamate, osteopontin, prostaglandin D synthase, prostatic binding protein, or ribosomal protein L17 also related with the pathogenesis of MS (Steinman and Zamyil. 2003). Especially, it was found that osteopontin was overexpressed on macrophages, microglia and astrocytes in human MS (Chabas et al. 2001) and osteopontin knockout mice were protected from severe EAE (Braitich and Constantinescu. 2010).

Progranulin (PGRN), also known as acrogranin, granulin-epithelin precursor, proepithelin, PC-cell-derived growth factor, and epithelial transforming growth factor, is a secreted N-linked glycoprotein consisting of tandem

repeats of a 12-cysteine module called the granulin or epithelin domain (Toh and Chitramuthu. 2011). It is a multifunctional protein implicated regeneration, wound repair, and inflammation in peripheral tissues such as lymphoid tissue, gastrointestinal mucosa, spleen, and skin epithelium (He and Bateman A. 2003; Daniel et al. 2000). PGRN can be degraded approximately 6 kDa peptides, called granulins (GRN) or epithelins by proteolytic enzymes such as elastase and proteinase-3 from neutrophils (Zhu et al. 2002; Kessenbrock et al. 2008; Toh and Chitramuthu. 2011). PGRN can regulate tumorigenesis including glioblastomas, and brain cancers (Liau et al. 2000; Menges et al. 2010). Furthermore, PGRN expression can enhance the growth of carcinomas of breast, ovary, endometrium, kidney, prostate, and bladder as well as non-epithelial cancers such as leiomyosarcomas and multiple myelomas (Toh and Bhitramuthu. 2011).

PGRN is reported to exist in the CNS such as osteopontin or glutamate. PGRN is expressed in neuronal and microglial populations and may function as an autocrine neuronal growth factor (Eriksen and Mackenzie. 2008). Especially, the mutation of the PGRN gene is widely known as a common cause of familial frontotemporal dementia (FTD) (Toh and Chitramuthu. 2011). The PGRN mutations was first identified in a large Canadian family with autosomal dominant FTD (Baker et al. 2006; Mackenzie et al. 2006). Hence, PGRN has been mainly studied in the relation to FTD (Baker et al. 2006; Mackenzie et al. 2006).

Meanwhile, several studies have reported the association between PGRN and autoimmune disease. PGRN is overexpressed in the patients of human inflammatory bowel disease (IBD) and its animal model induced by 3% dextran sodium sulfate (DSS) (Wei et al. 2014). The elevated serum concentration of PGRN is observed in rheumatoid arthritis (RA) patients (Yamamoto et al. 2014). In addition, PGRN prevents inflammation via inhibiting TNF- α activated intracellular signaling in collagen-induced arthritis animal model (Tang et al. 2011).

Therefore, PGRN knockout (PGRN^{-/-}) mice have been widely used for understanding the various roles of PGRN. PGRN^{-/-} mice were first generated for elucidating the association between sexual dimorphic behaviors and PGRN gene in 2007 (Kayasuga et al. 2007). PGRN^{-/-} mice used in this study were generated using Cre/loxP recombination system by Ding A's group in 2009 (Yin et al. 2009). Messenger ribonucleic acid (mRNA) levels of PGRN in these mice were undetectable in the intestines, spleen, skin, liver, kidney, and brain and they were healthy and fertile (Yin et al. 2009).

Therefore, to elucidate the potential role of PGRN in EAE, we determined the expression of PGRN in the CNS and the effects of PGRN deficiency during EAE progression using PGRN^{-/-} mice in the present study.

3. MATERIALS AND METHODS

Animals

All animal usage and protocols were reviewed and approved by Jeju National University Institutional Animal Care and Use Committee (accreditation No. 2015-0027). 8-week-old female C57BL/6 mice weighing 18-20g were obtained from Orientbio Inc. (Sungnam, Gyeonggido, Korea) and used for wild type (WT) mice. Homozygous B6(Cg)-Grn^{tm1.1AiDi}/J (Grn^{-/-}, also known as PGRN^{-/-}, The Jackson Laboratory, <https://www.jax.org/strain/013175>, Sacramento, CA, USA) were purchased and maintained in our facility. All mice were maintained under controlled light (lights on, 05:00-19:00), temperature (23±1°C), and humidity (55±10%) and given free access to food and water in accordance with the guidelines of the Care and Use of Laboratory Animals of the Institutional Ethical Committee of Jeju National University. In all cases, animal were euthanized and sacrificed by diethyl ether.

Induction and assessment of EAE

8-week-old female mice (WT and PGRN^{-/-}) were used for the induction of EAE. Each mouse received 200µg of MOG₃₅₋₅₅ peptide (M-E-V-G-W-Y-R-S-P-F-S-R-V-V-H-L-Y-R-N-G-K, purity>95%, GL Biochem (Shanghai) Ltd., Minhang, Shanghai, China) emulsified in complete Freund's adjuvant (CFA; BD

Difco™, Detroit, MI, USA) containing 500µg of heat-inactivated *Mycobacterium tuberculosis* (BD Difco™) by subcutaneous injection (s.c.) into the upper and lower back. Supplemental intravenous (i.v.) injections of 200ng of pertussis toxin (PT; List Biological Laboratories Inc., Campbell, CA, USA) were given on the same day and two days later. Clinical symptoms were monitored daily and clinical assessment of EAE was as follows: 0, no clinical signs; 1, flaccid tail; 2, hind limb weakness or abnormal gait; 3, complete hind limb paralysis; 4, complete hind limb paralysis with forelimb weakness or paralysis; 5, moribund or deceased (Sean Riminton et al. 1998).

Preparation of tissue and histological grading

Spinal cords were collected during the peak and recovery phases of EAE, respectively. Experimental mice of each group were sacrificed under the diethyl ether anesthesia and spinal cords were fixed in 10% neutral formalin and embedded in paraffin to obtain 3 µm paraffin sections. Hematoxylin and eosin (H&E) staining were used for routine histology and visualization of inflammation. The grade of inflammation was analyzed with 3 to 4 areas per tissue section of each mouse at x100 magnification and expressed as mean ± standard error (SE). Histological findings were graded into four categories (1, leptomeningeal infiltration; 2, mild perivascular cuffing; 3, extensive perivascular cuffing; 4, extensive perivascular cuffing and severe parenchymal cell infiltration) (Sakuma et al. 2004).

Immunohistochemistry

For detection of the immunoreactivity of PGRN, sections were deparaffinized and rehydrated using standard methods. Blocking reaction for endogenous peroxidase was performed by exposing sections in the 3% H₂O₂ solutions for 30 minutes and then incubated with normal goat serum 30 minutes for blocking unspecific bindings. Then sections were reacted with rabbit anti-mouse PGRN (1:200; Santa Cruz Biotechnology Inc., Dallas, TX, USA) antibody overnight at 4°C. Biotinylated goat anti-rabbit IgG followed by avidin-biotin-peroxidase complexes (ABC complexes; Vector Laboratories, Burlingame, CA, USA) were used as secondary antibodies. 3,3'-diaminbenzidine tetrachloride (DAB; Vector Laboratories) was used for detecting horseradish peroxidase (HRP) binding sites and counterstained with 2.5% Mayer's hematoxylin for 1 minute. Each slide was mounted with Canada balsam and analyzed with light microscope (LeicaDM LB2, Leica, Wetzlar, Germany). Quantifying positive cells stained by immunohistochemistry was done using Image J 1.48v software (National Institutes of Health (NIH), Bethesda, MD, USA).

Immunofluorescent staining

For immunofluorescent staining, sections were deparaffinized and rehydrated using standard methods. After incubation with normal goat serum and 5% of bovine serum albumin (BSA), tissue sections were reacted with the first antibody overnight at 4°C. The first antibodies used in the present study were

rabbit anti-mouse PGRN (1:50; Santa Cruz Biotechnology Inc.), mouse anti-mouse glial fibrillary acidic protein (GFAP, 1:500; Novus Biologicals LLC, Littleton, CO, USA), rabbit anti-mouse ionized calcium-binding adapter molecule-1 (Iba-1, 1:200; Wako Chemicals USA Inc., Richmond, VA, USA), rabbit anti-mouse cluster of differentiation (CD) 4 (1:10; biorbyt Ltd., Cambridge, Cambridgeshire, UK), rat anti-mouse CD8a (1:5; BioLegend, San Diego, CA, USA), and biotin anti-mouse CD11b (1:20, Biolegend). Secondary antibodies used for rabbit anti-mouse PGRN was biotin goat anti-rabbit IgG (1:100; Vector Laboratories) and then sections were finally incubated with streptavidin (STAV) conjugated tetramethylrhodamine (TRITC, 1:100; Jackson ImmunoResearch Laboratories Inc., West Grove, PA, USA). For other markers, fluorescein isothiocyanate (FITC) conjugated anti-mouse IgG (1:100; Santa Cruz Biotechnology, Inc.), Alexa Fluor[®] 488 conjugated anti-rabbit IgG (1:500; Thermo Fisher Scientific Inc., Waltham, MA, USA), or STAV conjugated Alexa Fluor[®] 488 (1:100; Jackson ImmunoResearch Laboratories Inc.) were used for secondary antibodies. After counterstained with 4', 6-diamidino-2-phenylindole dihydrochloride (DAPI, 1:2000; Sigma-Aldrich, St. Louis, MO, USA), the sections were mounted with the ProLong[®] Gold Antifade Reagent (Thermo Fisher Scientific Inc.). Each slide were examined under a fluorescent microscope (LeicaDM LB2, Leica) with appropriate filters. Images were taken using Olympus DP-72 microscope camera (Olympus, Tokyo, Japan) and merged using Adobe Photoshop[™] software.

Quantitative real-time polymerase chain reaction (real-time PCR)

Total spinal cord and spleen RNA was extracted with TRIZOL reagent (Ambion[®], Thermo Fisher Scientific Inc.). Two microgram of total RNA was reverse transcribed to 50ng/μl complementary deoxyribonucleic acid (cDNA) using reverse transcription system (Promega, Madison, WI, USA) and 10 ng of cDNA was used for PCR amplification. The expression of the genes encoding PGRN and glyceraldehyde 3-phosphate dehydrogenase (GAPDH) was quantified using SYBR Green PCR master mix (Applied Biosystems[®], Thermo Fisher Scientific Inc.) on an ABI StepOnePlus[™] (Applied Biosystems[®]) according to the manufacturer's instructions. Primer sequences are shown in Table 1. GAPDH was used as an internal control and a PCR negative control were included. Relative gene expression levels were calculated according to the cycle threshold (Ct) values of target genes and normalized to the expression of the internal control gene using the REST program (Qiagen, Hilden, Germany).

Western Blot

To evaluate the expression patterns of PGRN, frozen spinal cord tissue was thawed and homogenized in a TNN buffer consisting of 40 mM Tris-HCl, pH 7.4, and 120 mM NaCl containing the protease inhibitors (1 mM phenylmethylsulfonyl fluoride (PMSF), 10 μg/ml leupeptin, 10 μg/ml aprotinin, and 2 mM Na₃VO₄). Equal amounts of protein (40 μg/well) were loaded onto

8.5% sodium dodecyl sulfate polyacrylamide gel electrophoresis (SDS-PAGE) gels and immunoblotted onto a nitrocellulose membrane (GE Healthcare, Milwaukee, WI, USA). For blocking, the membrane were incubated with 2% skim milk for 1 hour. Then, the membrane were incubated with antibodies against rabbit anti-mouse PGRN (1:1000; Santa Cruz Biotechnology Inc.) or mouse anti-mouse β -actin (1:2000; Sigma-Aldrich) overnight at 4°C. After incubation with HRP conjugated anti-mouse or rabbit IgG (1:2000; Invitrogen™, Thermo Fisher Scientific), the blots were developed by enhanced chemiluminescence reagents (ECL; Cyanagen Srl, Bologna, Italy) and the images of each band were obtained using Fusion Solo (Vilber Lourmat, Eberhardzell, Germany). The densities of bands were analyzed with Image J 1.48v software (NIH, Bethesda, MD, USA).

Cell culture and proliferation assay

For proliferation assay, spleen mononuclear cells were isolated from each mice at disease peak and suspended in RPMI-1640 medium (Gibco, Paislye, UK) supplemented with 10% (v/v) fetal bovine serum (FBS; Gibco), 100U/ml penicillin-streptomycin (P/S; Gibco), 1% 4-(2-hydroxyethyl)-1-piperazineethanesulfonic acid (HEPES; Gibco), 1% sodium pyruvate (Gibco), 1% non-essential amino acid (NEAA; Gibco), and 0.055 mM beta-mercaptoethanol (β -ME; Gibco). To perform proliferation assay, spleen mononuclear cells were seeded at a density of 4×10^5 cells/well onto 96-well microtiter plate (Nunc®,

Sigma-Aldrich) in triplicate with or without MOG₃₅₋₅₅ peptide (10 µg/ml), PLP₁₃₉₋₁₅₁ peptide (5 µg/ml) or concanavalin A (Con A) (5 µg/ml; Sigma) at 37°C in 5% CO₂ for 54 hours. 1 µCi of ³H-thymidine (specific activity 42 Ci/mmol; Amersham, Arlington Heights, IL, USA) were added to each well. After incubation for 18 hours, cells were harvested onto glass fiber filters by using an automatic cell harvester and the amount of thymidine uptaken into DNA was analyzed by liquid scintillation spectrometer (Wallac Micro Beta[®] TriLux, Perkin Elmer, Waltham, MA, USA). Stimulation with Con A was used as a positive control.

Statistical analyses

Statistical analysis of each result was performed using One-way analysis of variance (ANOVA) followed by Tukey's HSD test. The results were presented as the mean and respective SE for each group. Clinical scores and histological score were analyzed using the non-parametric Mann-Whitney U-test. A *p* value <0.05 was considered statistically significant.

4. RESULTS

The expression of PGRN was important to the disease process of EAE

To investigate the change of PGRN expression in the neuroinflammatory process associated with EAE, real-time PCR and western blot analysis were performed with the spinal cords of EAE mice in different clinical phases (Fig. 1A, days 16 and days 30 p.i. represent at the disease peak and recovery, respectively. As EAE progressed, the mRNA expression of PGRN significantly increased compared with naïve control mice, especially at the disease peak (Fig. 1B, *** $p < 0.005$). In addition, western blot analysis showed significantly increased protein expression of PGRN in EAE, especially at the disease peak (Fig. 1C-E). It was reported that the 88kDa bands were the secretory form of the fully glycosylated isoform of PGRN and the 58-68kDa bands were the pre-secretory form of the glycosylated immature isoform of PGRN (Kanazawa et al. 2015). In present study, both forms of PGRN especially increased at the disease peak (Fig. 1D-E). This results suggested that the expression of PGRN is important to the disease progress of EAE.

PGRN was overexpressed in the glial cells and inflammatory cells

The localization of PGRN in the spinal cords was determined by immunohistochemistry (Fig. 2 and Table 2). The expression of PGRN was markedly higher in EAE mice rather than naïve mice. At the disease peak,

immunoreactivity of PGRN was mainly observed in inflammatory cells of perivascular clusters (Fig. 2B, and E) and activated glial cells around inflammatory lesions (Fig. 2H, 2K). At the disease recovery, immunoreactivity of PGRN was observed in some glial cells around inflammatory lesions (Fig 2C, F, I, and L). Quantification of PGRN positive cells by Image J software showed that PGRN positive cells were significantly increased at the disease peak and recovery compared to naïve control mice (Fig 2M, *** $p < 0.005$). Double immunofluorescence staining revealed that PGRN immunoreactivity was co-localized with GFAP (Fig. 3), Iba-1 (Fig. 4), CD4, CD8 and CD11b (Fig. 5). These observations indicated that PGRN was expressed by astrocytes (GFAP⁺), microglia (Iba-1⁺), CD4⁺ T cells, CD8⁺ T cells, and CD11b⁺ macrophages in the CNS during EAE.

PGRN depletion protects mice against EAE

Next, we tested whether depletion of PGRN could modulate EAE progression using PGRN^{-/-} mice immunized with MOG₃₅₋₅₅ in CFA. Clinical evaluation indicated that PGRN depletion significantly reduced the severity and incidence of EAE (Fig 6 and Table 3). In WT EAE mice, all mice showed symptoms (100%, 8/8 animals) and the maximal score was 2.4 ± 0.16 . In contrast, the incidence of PGRN^{-/-} EAE mice (63%, 5/8 animals) were lower and the maximal score was attenuated to 0.8 ± 0.35 compared to that of WT EAE mice (*** $p < 0.005$).

PGRN depletion inhibited the infiltration of inflammatory cells

Consistent with these clinical findings, H&E staining was performed for histopathological examination of the spinal cords of WT EAE and PGRN^{-/-} EAE mice at the disease peak. WT EAE mice showed a broad distribution of inflammatory cells in the perivascular lesions (Fig. 7A and B) and the subpial space (Fig. 7C and D). By contrast, PGRN^{-/-} EAE mice manifested markedly decreased infiltration of inflammatory cells in the perivascular lesions (Fig. 7E and F) and the subarachnoid space (Fig 7G and H). The mean histological scores were 2.4 ± 0.24 in WT EAE and 0.5 ± 0.32 in PGRN^{-/-} EAE mice (Fig. 7I, ** $p < 0.01$). Taken together, these results suggested that the depletion of PGRN significantly ameliorated the neuroinflammation in the CNS during EAE.

PGRN depletion impaired T cell responses in periphery

Then we tested antigen-specific T cell proliferation in PGRN^{-/-} EAE mice. ³H-thymidine incorporation in splenic mononuclear cells (MNCs) revealed that the proliferation of antigen-specific splenic MNCs in response to MOG₃₅₋₅₅ peptide significantly increased in WT EAE mice compared with PGRN^{-/-} EAE mice (Fig. 8). In contrast, neither splenic MNCs of WT EAE mice nor PGRN^{-/-} EAE mice showed difference in cell proliferation when stimulated with PLP, a neuroantigen which shows different genetic susceptibility. Taken together, these results indicated that splenic MNCs of PGRN^{-/-} EAE mice could modulate MOG₃₅₋₅₅ specific autoreactive T cells.

5. DISCUSSION

In the present study, the expression levels of PGRN and the cell types expressing PGRN were elucidated in the CNS of EAE mice presenting different clinical phases. Next, we found that PGRN was involved in using PGRN^{-/-} mice.

EAE is the most widely used animal model for the human MS. EAE is characterized by inflammation and demyelination of the CNS as MS. It is commonly recognized that myelin-reactive inflammatory cells such as autoreactive T cells or macrophages infiltrate into the CNS during EAE progression (Bauer et al. 1995). In addition, neurotransmitters such as glutamate and osteopontin also related with the pathogenesis of MS (Steinman and Zamyil. 2003). The expression of osteopontin was increased on macrophages, microglia and astrocytes in human MS and activated glial cells in EAE (Chabas et al. 2001; Park et al. 2006). The expression of glutamate is also known to increase in CSF and brain of MS patients (Centonze et al. 2010). However, although several studies have proposed the relationship between the neurotransmitters and MS/EAE pathogenesis, few studies have looked at transcriptional profiles in MS lesions (Steinman and Zamyil. 2003).

PGRN is a secreted glycoprotein and expressed in cells with a high mitotic rate in lymphoid tissue, spleen, gastrointestinal mucosa, and skin epithelium (Eriksen and Mackenzie. 2008). Secreted PGRN in peripheral tissue has been reported to influence tissue repair, wound healing, systemic inflammation

process or tumor growth (Eriksen and Mackenzie. 2008). In the CNS, PGRN is also expressed on neuronal and microglial populations similarly to osteopontin or glutamate (Petkau and Leavitt. 2014). PGRN mRNA is expressed in the forebrain, olfactory bulbs, and spinal cord (Daniel et al. 2003).

In the CNS, the mutation of the PGRN gene have been identified to cause FTD (Toh and Chitramuthu. 2011) and elevated mRNA levels of PGRN has been observed in inflammatory neurodegenerative disorders associated with microglial activation (Wada et al. 2000) and Alzheimer's disease (Pereson et al. 2009). In addition, the elevated PGRN protein levels have been linked to the occurrence of brain cancers such as gliomas and intracranial meningiomas (Menges et al. 2010). Meanwhile, the potential roles of PGRN in several autoimmune diseases such as IBD and RA have been reported (Wei et al. 2014; Yamamoto et al. 2014). The overexpression of PGRN was observed in human IBD and its animal model (Wei et al. 2014). In addition, the serum concentration of PGRN was increased in RA patients and PGRN prevented inflammation via inhibiting TNF- α signaling pathway in its animal model (Tang et al. 2011). Therefore, we hypothesized that PGRN might be related with EAE, a neurodegenerative autoimmune disease.

There are only two conflicting opinions of the expression of PGRN in MS. One group has reported no significant difference of PGRN levels in MS (De Riz et al. 2010), however, another group has found elevated expression levels of PGRN in the brain of MS patients (Vercellino et al. 2011). Few studies have

looked at the effect of PGRN on MS/EAE pathogenesis. So, we aimed to determine the association between PGRN and EAE progression. First, we found that mRNA and protein levels of PGRN are elevated in the CNS of EAE-affected mice. These results are in agreement with the prior study of Vercellino's group. Furthermore, we also elucidated that PGRN is mainly expressed on astrocytes, microglia and infiltrated CD4⁺ T cells, CD8⁺ T cells, and CD11b⁺ macrophages in the CNS of EAE mice.

Next, it was tested that deficient of PGRN gene could influence the EAE progression using PGRN^{-/-} mice and dramatically reduced EAE clinical sign and neuroinflammation in PGRN^{-/-} EAE mice were observed. In accordance with these results, antigen-specific T cell proliferation in PGRN^{-/-} EAE mice was significantly decreased compared with WT EAE mice.

Taken together, these findings suggest that PGRN might be related with EAE progression. In peripheral tissue, the role of PGRN during inflammation is mediated by interaction with elastase and secretory leukocyte protease inhibitor (SLPI) (Zhu et al. 2002; Kessenbrock K et al. 2008). PGRN and GRNs show the opposing effects on inflammatory process (Toh and Chitramuthu, 2011). When elastase secreted by neutrophils cleaves PGRN to release GRNs, GRNs promote inflammation process (HE et al. 2003). However, if cleavage of PGRN by the proteolytic enzymes such as elastase or proteinase-3 is inhibited by SLPI secreted by neutrophils and macrophages, PGRN tends to suppress inflammatory process (Zhu et al. 2002; Kessenbrock K et al. 2008). Actually,

there is currently limited information about the role of PGRN in CNS inflammation (Eriksen and Mackenzie. 2008). Several studies have reported that astrocytes can release SLPI, and cultured microglia can secrete elastase (Nakajima et al. 1992; Zhu et al. 2002). So, PGRN in CNS is likely to serve a similar role in peripheral tissue (Eriksen and Mackenzie. 2008). However, the inhibition of SPLI ameliorated clinical symptoms in EAE (Muller et al. 2012) despite the anti-inflammatory effect of SPLI related with PGRN. Therefore, further studies are needed for elucidating ameliorated EAE in PGRN^{-/-} mice interacting with enzyme activities related with the cleavage of PGRN.

Although we cannot pinpoint the mechanism, these results indicate that PGRN could contribute to the disease and may have potential as a therapeutic agent against EAE/MS. It also suggests possible biological connection between PGRN and EAE warranting further exploration of its involvement in the pathogenesis of MS.

6. REFERENCES

- Bauer J, Huitinga I, Zhao W, Lassmann H, Hickey WF, Dijkstra CD. 1995. The role of macrophages, perivascular cells, and microglial cells in the pathogenesis of experimental autoimmune encephalomyelitis. *Glia* 15(4):437-43.
- Baxter AG. 2007. The origin and application of experimental autoimmune encephalomyelitis. *Nat Rev Immunol* 7(11):904-12.
- Braithwaite M, Constantinescu CS. 2010. The role of osteopontin in experimental autoimmune encephalomyelitis (EAE) and multiple sclerosis (MS). *Inflamm Allergy Drug Targets* 9(4):249-56.
- Centonze D, Muzio L, Rossi S, Furlan R, Bernardi G, Martino G. 2010. The link between inflammation, synaptic transmission and neurodegeneration in multiple sclerosis. *Cell Death Differ* 17(7):1083-91.
- Chabas D, Baranzini SE, Mitchell D, Bernard CC, Rittling SR, Denhardt DT, Sobel RA, Lock C, Karpus M, Pedotti R, Heller R, Oksenberg JR, Steinman L. 2001. The influence of the proinflammatory cytokine, osteopontin, on autoimmune demyelinating disease. *Science* 294(5547):1731-35.
- Daniel R, Daniels E, He Z, Bateman A. 2003. Progranulin (acroganin/PC cell-derived growth factor/granulin-epithelin precursor) is expressed in the placenta, epidermis, microvasculature, and brain during murine

- development. *Dev Dyn* 227:593-99.
- De Riz M, Galimberti D, Fenoglio C, Piccio LM, Scalabrini D, Venturelli E, Pietroboni A, Piola M, Naismith RT, Parks BJ, Fumagalli G, Bresolin N, Cross AH, Scarpini E. 2010. Cerebrospinal fluid progranulin levels in patients with different multiple sclerosis subtypes. *Neurosci Lett* 469(2):234-6.
- Eriksen JL, Mackenzie IR. 2008. Progranulin: normal function and role in neurodegeneration. *J Neurochem* 104(2):287-97.
- He Z, Bateman A. 2003. Progranulin (granulin-epithelin precursor, PC-cell-derived growth factor, acrogranin) mediates tissue repair and tumorigenesis. *J Mol Med (Berl)* 81:600-12.
- Kanazawa M, Kawamura K, Takahashi T, Miura M, Tanaka Y, Koyama M, Toriyabe M, Igarashi H, Nakada T, Nishihara M, Nishizawa M, Shimohata T. 2015. Multiple therapeutic effects of progranulin on experimental acute ischaemic stroke. *Brain* 138:1932-48.
- Kayasuga Y, Chiba S, Suzuki M, Kikusui T, Matsuwaki T, Yamanouchi K, Kotaki H, Horai R, Iwakura Y, Nishihara M. 2007. Alteration of behavioural phenotype in mice by targeted disruption of the progranulin gene. *Behav Brain Res* 185(2):110-8.
- Kessenbrock K, Fröhlich L, Sixt M, Lämmermann T, Pfister H, Bateman A, Belaouaj A, Ring J, Ollert M, Fässler R, Jenne DE. 2008. Proteinase 3 and neutrophil elastase enhance inflammation in mice by inactivating anti-

- inflammatory progranulin. *J Clin Invest* 118(7):2438-47.
- Liau LM, Lallone RL, Seitz RS, Buznikov A, Gregg JP, Kornblum HI, Nelson SF, Bronstein JM. 2000. Identification of a human glioma-associated growth factor gene, granulin, using differential immuno-absorption. *Cancer Res* 60(5):1353-60.
- Mackenzie IR, Baker M, West G, Woulfe J, Qadi N, Gass J, Cannon A, Adamson J, Feldman H, Lindholm C, Melquist S, Pettman R, Sadovnick AD, Dwosh E, Whiteheart SW, Hutton M, Pickering-Brown SM. 2006. A family with tau-negative frontotemporal dementia and neuronal intranuclear inclusions linked to chromosome 17. *Brain* 129(Pt 4):3081-90.
- Martin R, McFarland HF. 1995. Immunological aspects of experimental allergic encephalomyelitis, multiple sclerosis. *Crit Rev Clin Lab Sci* 32:121-82.
- Menges CW, Chen Y, Mossman BT, Chernoff J, Yeung AT, Testa JR. 2010. A phosphotyrosin proteomic screen identifies multiple tyrosine kinase signaling pathways aberrantly activated in malignant mesothelioma. *Genes Cancer* 1:493-505.
- Müller AM, Jun E, Conlon H, Sadiq SA. 2012. Inhibition of SLPI ameliorates disease activity in experimental autoimmune encephalomyelitis. *BMC Neurosci* 13:30.
- Nakajima K, Shimojo M, Hemanoue M, Ishiura S, Sugita H, Kohsaka S. 1992. Identification of elastase as a secretory protease from cultured rat microglia. *J Neurochem* 58(4):1401-08.

- Park S, Hwang I, Kim G, Shin T, Jee Y. 2006. Increased osteopontin expression in activated glial cells in experimental autoimmune encephalomyelitis. *Korean J Vet Res* 46(3):177-84.
- Pereson S, Wils H, Kleinberger G, McGowan E, Vandewoestyne M, Van Broeck B, Joris G, Cuiit I, Deforce D, Hutton M, Van Broeckhoven C, Kumar-Singh S. 2009. Progranulin expression correlates with dense-core amyloid plaque burden in Alzheimer disease mouse models. *J Pathol* 219(2):173-81.
- Petkau TL, Leavitt BR. 2014. Progranulin in neurodegenerative disease. *Trends Neurosci* 37(7):388-98.
- Sakuma H, Kohyama K, Park IK, Miyakoshi A, Tanuma N, Matsumoto Y. 2004. Clinicopathological study of a myelin oligodendrocyte glycoprotein-induced demyelinating disease in LEW.1AV1 rats. *Brain* 127(Pt 10):2201-13.
- Sean Riminton D, Kórner H, Strickland DH, Lemckert FA, Pollard JD, Sedgwick JD. 1998. Challenging cytokine redundancy: inflammatory cell movement and clinical course of experimental autoimmune encephalomyelitis are normal in lymphotoxin-deficient, but not tumor necrosis factor-deficient, Mice. *J Exp Med* 187(9):1517-28.
- Steinman L. 1999. Assessment of animal models for MS and demyelinating disease in the design of rational therapy. *Neuron* 24(3):511-4.
- Steinman L, Zamvil S. 2003. Transcriptional analysis of targets in multiple

- sclerosis. *Nat Rev Immunol* 3(6):483-92.
- Stinissen P, Medaer R, Raus J. 1998. Myelin reactive T cells in the autoimmune pathogenesis of multiple sclerosis. *Mult Scler* 4(3):203-11.
- Tang W, Lu Y, Tian QY, Zhang Y, Guo FJ, Liu GY, Syed NM, Lai Y, Lin EA, Kong L, Su J, Yin F, Ding AH, Zanin-Zhorov A, Dustin ML, Tao J, Craft J, Yin Z, Feng JQ, Abramson SB, Yu XP, Liu CJ. 2011. The growth factor progranulin binds to TNF receptors and is therapeutic against inflammatory arthritis in mice. *Science* 332(6028):478-84.
- Toh H, Chitramuthu BP. 2011. Structure, function, and mechanism of progranulin; the brain and beyond. *J Mol Neurosci* 45:538-48.
- Vercellino M, Grifoni S, Romagnolo A, Masera S, Mattioda A, Trebini C, Chiavazza C, Caligiana L, Capello E, Mancardi GL, Giobbe D, Mutani R, Giordana MT, Cavalla P. 2011. Progranulin expression in brain tissue and cerebrospinal fluid levels in multiple sclerosis. *Mult Scler* 17(10):1194-1201.
- Wada R, Tiffit CJ, Proia RL. 2000. Microglial activation precedes acute neurodegeneration in Sandhoff' disease and is suppressed by bone marrow transplantation. *Proc Natl Acad Sci USA* 97:10954-59.
- Wei F, Zhang Y, Jian J, Mundra JJ, Tian Q, Lin J, Lafaille JJ, Tang W, Zhao W, Yu X, Liu CJ. 2014. PGRN protects against colitis progression in mice in an IL-10 and TNFR2 dependent manner. *Sci Rep* 4:7023.
- Yamamoto Y, Takemura M, Serrero G, Hayashi J, Yue B, Tsuboi A, Kubo H,

- Mitsuhashi T, Mannami K, Sato M, Matsunami H, Matuo Y, Saito K. 2014. Increased serum GP88 (progranulin) concentrations in rheumatoid arthritis. *37(5):1806-13.*
- Yin F, Banerjee R, Thomas B, Zhou P, Gian L, Jia T, Ma X, Ma Y, Iadecola C, Beal MF, Nathan C, Ding A. 2009. Exaggerated inflammation, impaired host defense, and neuropathology in progranulin-deficient mice. *J Exp Med 207(1):117-28.*
- Zhu J, Nathan C, Jin W, Sim D, Ashcroft GS, Wahl SM, Lacomis L, Erdjument-Bromage H, Tempst P, Wright CD, Ding A. 2002. Conversion of proepithelin to epithelins: roles of SLPI and elastase in host defence and wound repair. *Cell 111(5):867-78.*

7. Tables

Table 1. Primers sequences for PGRN and GAPDH

Gene	Primer sequence
PGRN	Forward 5'-TTCACACACGATGCGTTTCA-3'
	Reverse 5'-AGGGCACACAGAAAAAG-3'
GAPDH	Forward 5'-TACCCCAATGTGTCCGTC-3'
	Reverse 5'-AAGAGTGGGAGTTGCTGTTGAG-3'

Abbreviations: PGRN, progranulin; GAPDH, glyceraldehyde 3-phosphate dehydrogenase

Table 2. Immunoreactivity of PGRN on various cells in spinal cords

Cell type	Group		
	Naïve	Peak	Recovery
Glial cells	+	+++	++
Inflammatory cells	-	+++	+/-

Immunohistochemistry was performed on spinal cord of naïve mice and EAE mice at disease peak and recovery. Results shows intensity of PGRN immunoreactivity on various cells as follows: -, negative; +, < 10 cells; ++, <20 cells; +++, < 40 cells under magnification x200.

Table 3. Summary of active clinical parameters

Group	Clinical status		
	Incidence (%)	Days of onset	Mean of maximal score
WT EAE	100 (8/8)	13.4 ± 0.81	2.4 ± 0.16
PGRN ^{-/-} EAE	63 (5/8)	14.2 ± 0.48	0.8 ± 0.35***

WT and PGRN^{-/-} mice were inoculated with MOG₃₅₋₅₅ peptide to induce EAE. Results are the mean values ± SE. The difference in mean of maximal scores between WT EAE and PGRN^{-/-} EAE mice were statistically significant. *** $p < 0.005$, significantly different by Mann-Whitney test.

8. Figures

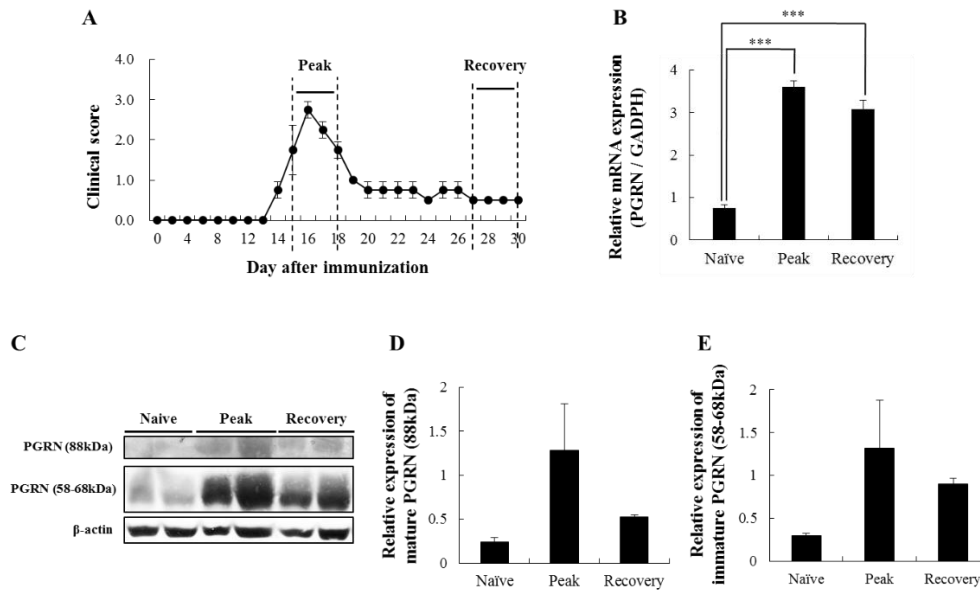


Figure 1. Disease symptom scores and relative expression of PGRN in EAE mice. (A) C57BL/6 mice were immunized with MOG₃₅₋₅₅ mixed in CFA and the development of EAE was observed daily. (B) Real-time PCR on cDNA extracted from spinal cords of naïve or EAE mice was performed with PGRN primers. mRNA expression of PGRN were normalized relative to that of GAPDH. (C) PGRN expression in spinal cord was estimated in the peak and recovery phases of EAE. (D) The expression level of mature PGRN (88kDa) was normalized against that of β -actin. (E) The expression level of immature PGRN (58-68kDa) was normalized against that of β -actin. *** $p < 0.005$ compared to the naïve control by one-way ANOVA followed by Tukey's HSD test.

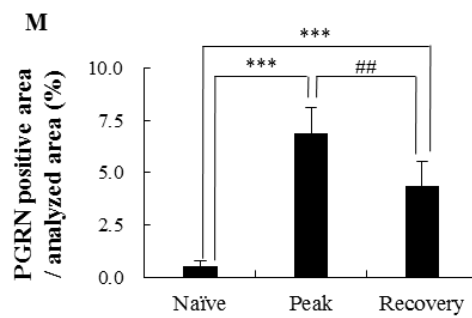
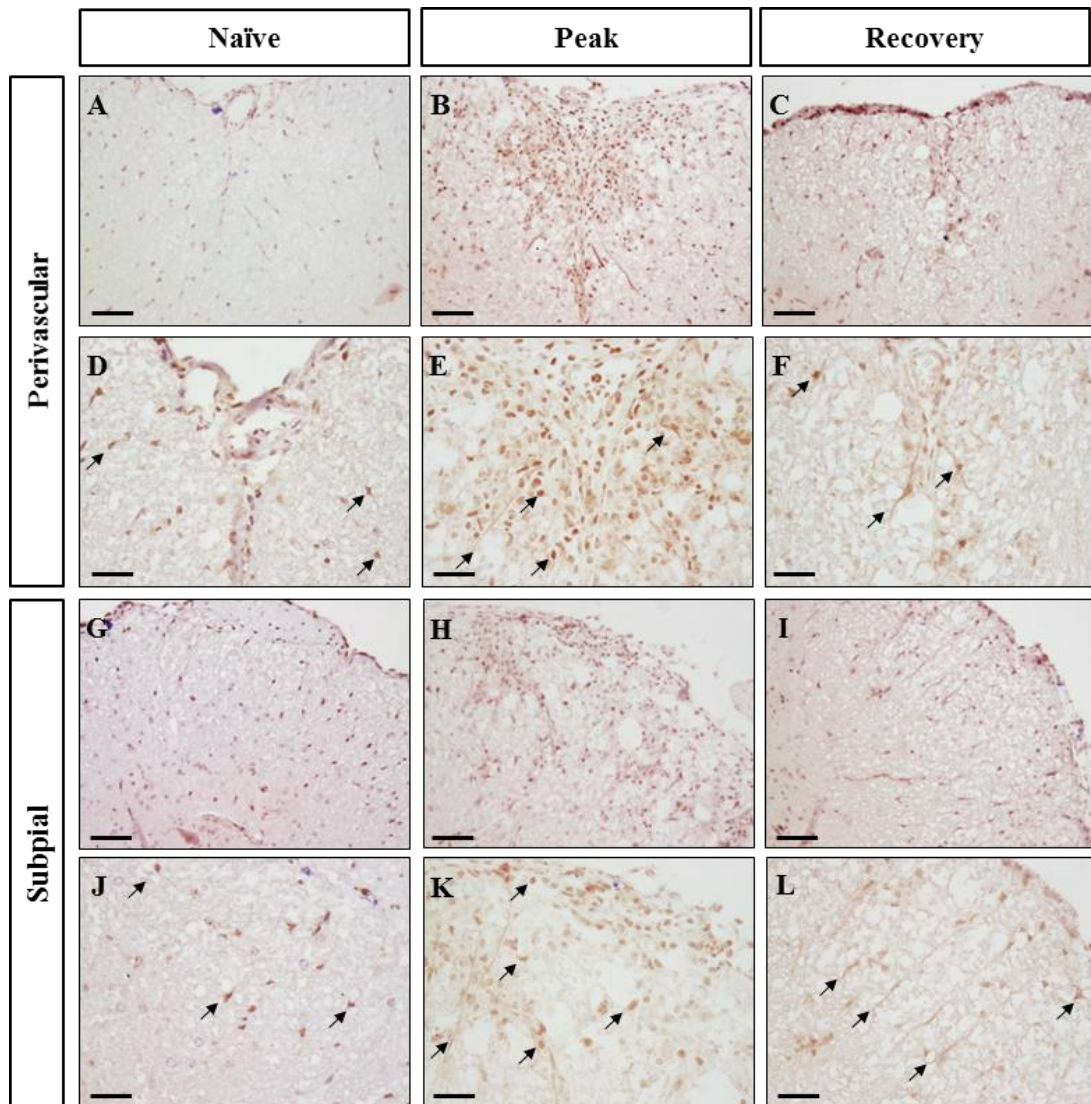


Figure 2. PGRN was overexpressed in glial cells and inflammatory cells of the spinal cord during EAE development. (A, D, G, J) Immunoreactivity of PGRN

was low in perivascular (A, D) and subpial regions (G, J) of the spinal cord of naïve mice. (B-C, E-F, H-I, K-L) During EAE, intense PGRN immunoreactivity was visualized in microglia, astrocytes, and infiltrated inflammatory cells of perivascular (B-C, E-F) and subpial regions (H-I, K-L) in the spinal cord. Arrows indicate positive cells for PGRN immunoreactivity. (M) Quantification of PGRN positive cells were performed using five lesions showing the most representative expression of each mouse (3 to 6 mice per group). Scale bars = 100 μm (A-C, G-I), 50 μm (D-F, J-L). *** $p < 0.005$ compared to the naïve mice, ## $p < 0.01$ compared to the peak stage of EAE mice by one-way ANOVA followed by Tukey's HSD test.

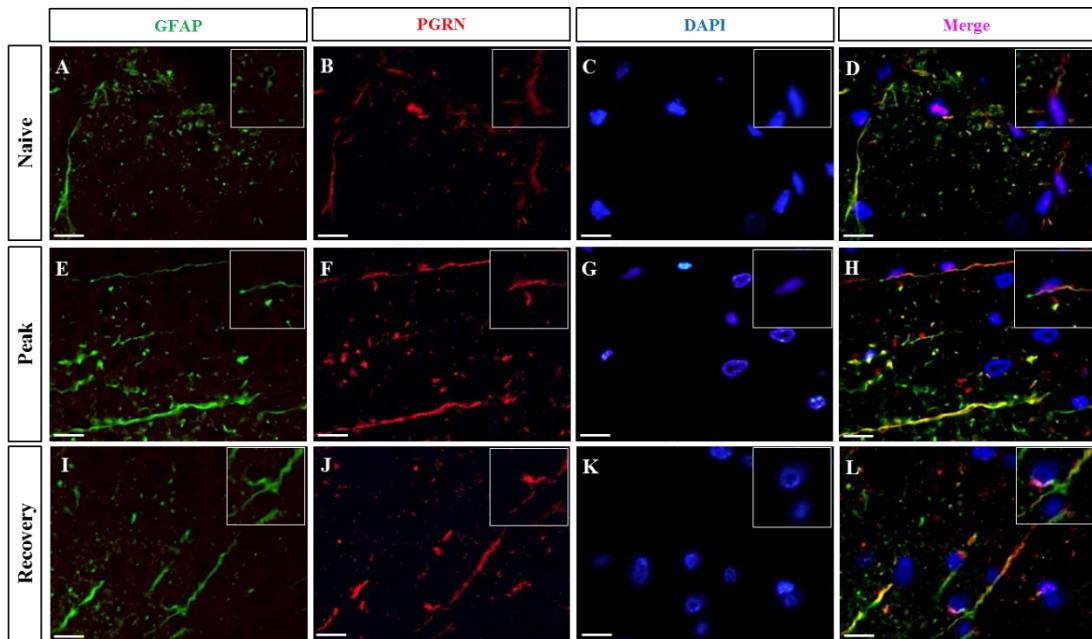


Figure 3. PGRN was overexpressed on astrocytes. Double fluorescence staining of GFAP (green) and PGRN (red) in the spinal cords of naïve and EAE mice. Images were merged (magenta) to compare co-localization of PGRN and GFAP in naïve control (A-D), peak (E-H), and recovery stage animals (I-L). Boxed areas are shown at higher magnification of double positive cell adjusted using Adobe Photoshop software. Scale bars = 25 μ m.

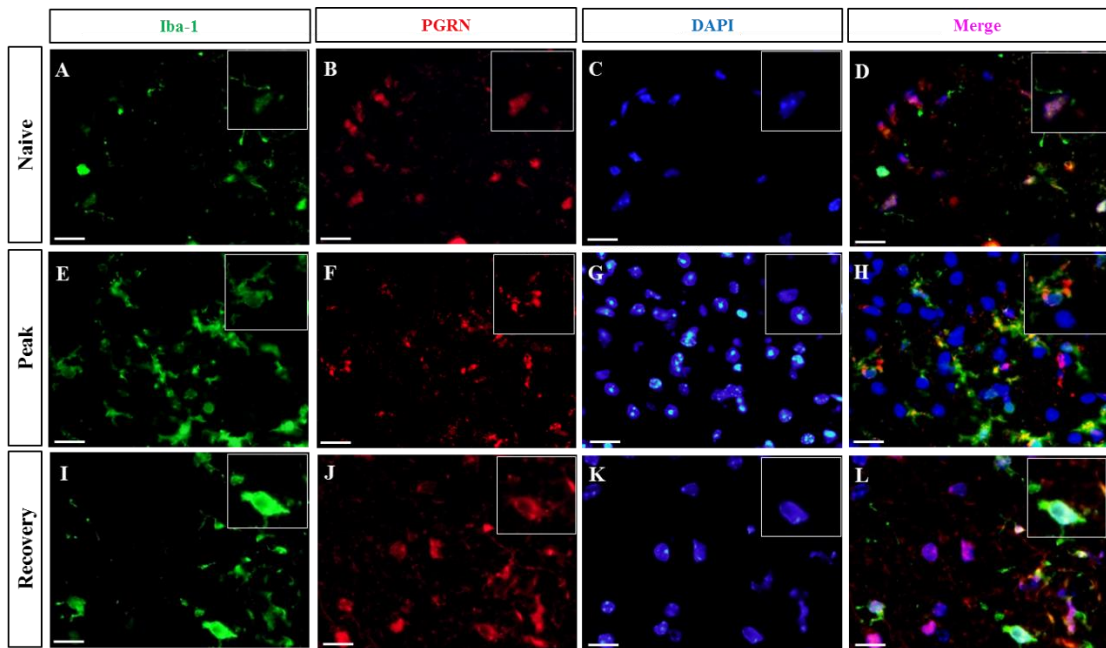


Figure 4. PGRN was overexpressed on microglia. Double fluorescence staining of Iba-1 (green) and PGRN (red) in the spinal cords of naïve and EAE mice. Images were merged (magenta) to compare co-localization of PGRN and Iba-1 in naïve control (A-D), peak (E-H), and recovery stage animals (I-L). Boxed areas are shown at higher magnification of double positive cell adjusted using Adobe Photoshop software. Scale bars = 25 μ m.

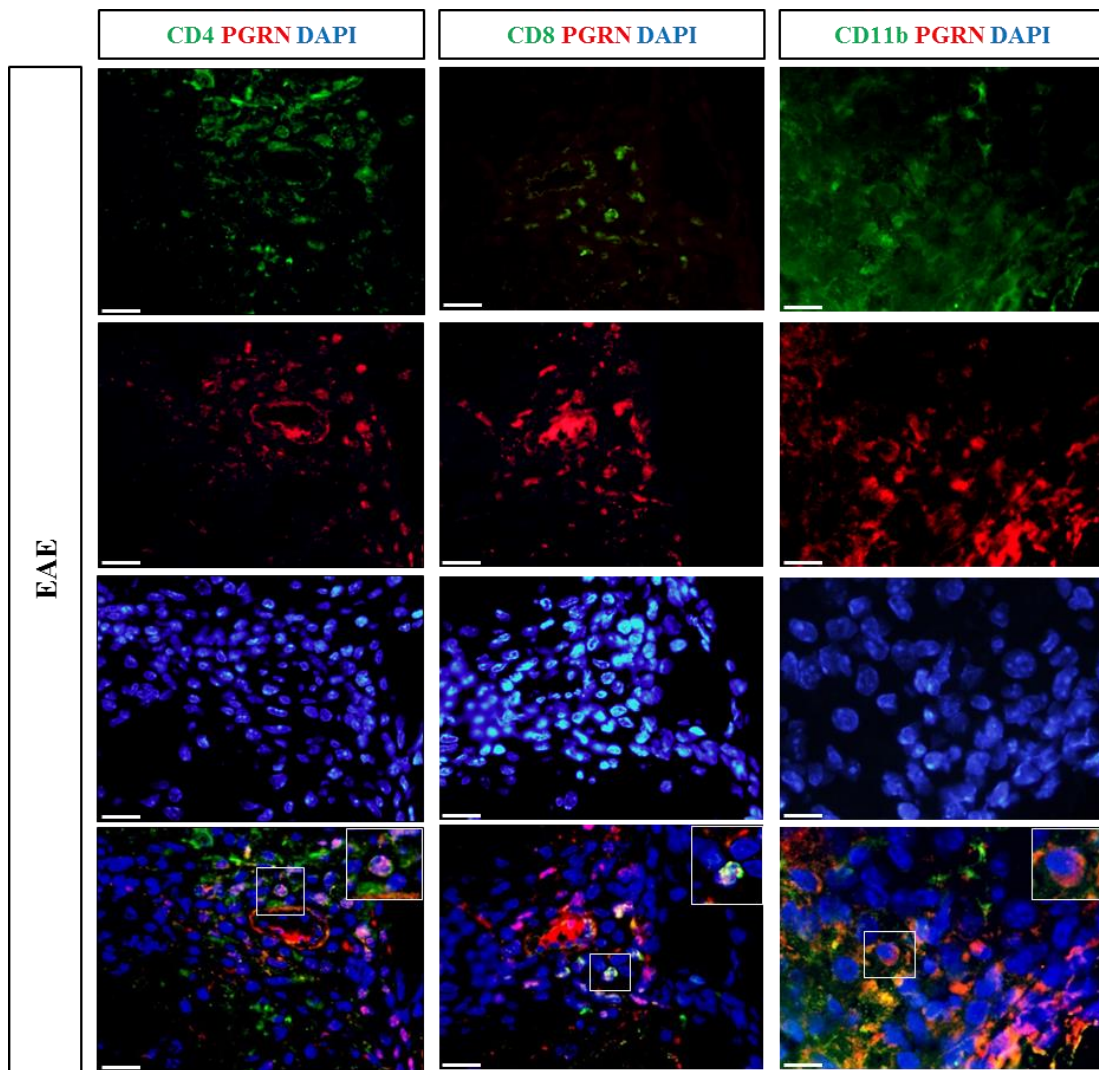


Figure 5. Double fluorescence staining revealed PGRN-positive CD4⁺ T cells, CD8⁺ T cells, and CD11b⁺ positive macrophages in the spinal cords of EAE mice. Boxed areas are shown at higher magnification of double positive cell adjusted using Adobe Photoshop software. CD4, CD8, CD11b; green, PGRN; red, nuclei; blue. Scale bars = 25 μ m.

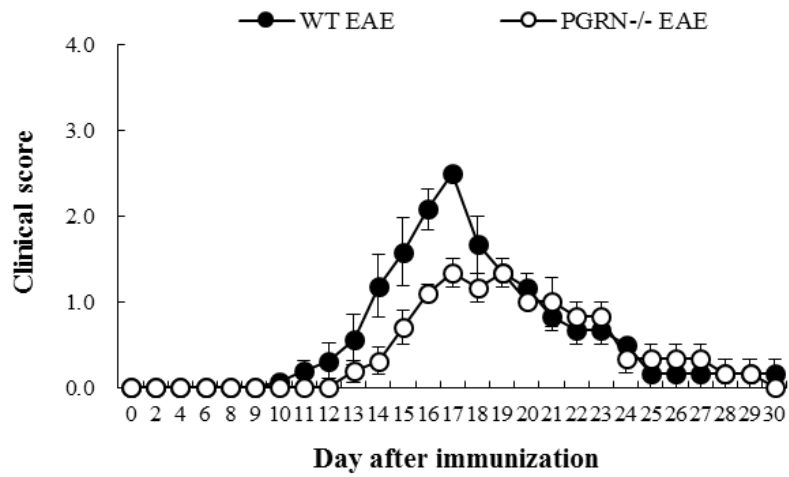


Figure 6. Clinical scores of MOG₃₅₋₅₅ induced EAE in WT and PGRN^{-/-} mice. PGRN depletion showed markedly ameliorated clinical symptoms. WT and PGRN^{-/-} mice were immunized with MOG₃₅₋₅₅ mixed in CFA and the development of EAE was observed daily.

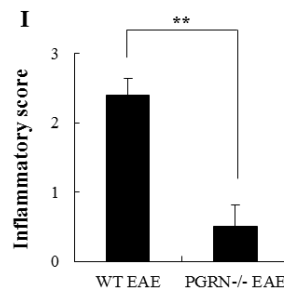
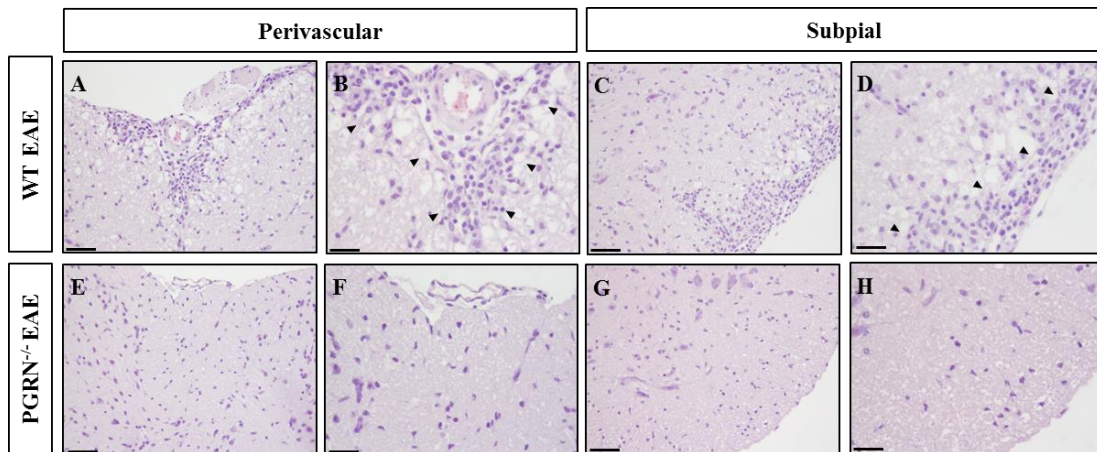


Figure 7. Infiltration of inflammatory cells into lumbar spinal cord sections obtained from WT EAE and PGRN^{-/-} EAE mice. PGRN depletion showed markedly ameliorated clinical symptoms and neuro-inflammation. Images B, D, F, and H are higher magnification of the images A, C, E, and G, respectively. (M) Quantification of inflammatory score of each group. Scale Bars = 100 μ m (A, C, E, and G), 50 μ m (B, D, F and H). ** $p < 0.01$ compared to the WT mice by student's *t*-test.

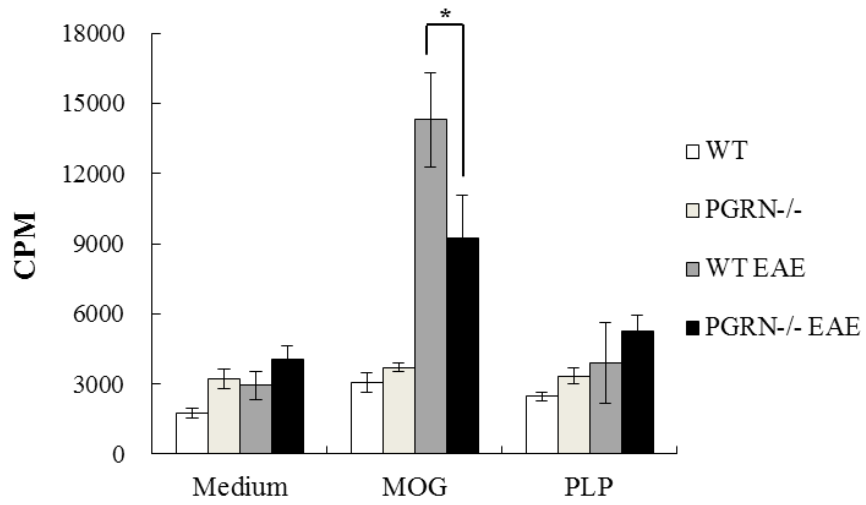


Figure 8. PGRN depletion impaired the proliferation of MOG₃₅₋₅₅ reactive splenic mononuclear cells. Splenic mononuclear cells were isolated from mice of each group and cultured in medium with or without MOG₃₅₋₅₅ peptides or PLP₁₃₈₋₁₅₁ peptides. * $p < 0.05$ compared to the WT EAE mice by one-way ANOVA followed by Tukey's HSD test.

신규 자가면역성 뇌척수염 치료제 표적으로써의 progranulin 역할

지도교수 : 지영훈

조진희

제주대학교 대학원 수의학과

사람의 다발성 경화증 (MS) 및 그 동물모델인 실험적 자가면역성 뇌척수염 (EAE)은 중추 신경계의 염증, 말이집 탈락 (demyelination), 아교세포흉터형성 (glial scarring)을 특징으로 하는 자가반응성 염증성 T세포 (autoreactive pro-inflammatory T cell) 매개성 질병으로 알려져있다. MS 및 EAE의 발병기전은 현재까지 정확하게 밝혀지지 않았지만, 자가반응성 T 세포 외에도 신경전달물질인 glutamate나 osteopontin등의 과발현에 의해서도 발생할 수 있다고 보고된바 있다. 한편, progranulin은 분비형 glycoprotein의 일종으로 체내의 여러 곳에서 발현하여 세포의 분열, 생존, 이주 등에 관여한다고 알려졌다. 특히, 여러 효소와의 상호 작용을 통해 분해가 되지 않은 형태는 염증 반응을 억제하지만, 단백질 가수 분해 효소에 의해 granulin의 형태로 분해되면 염증 반응을 오히려 촉진하여, 그 기능에서 양면성을 보인다고 보고되었다. Progranulin은 glutamate나 osteopontin 등과 같이 신경계 내 신경세포 및 미세아교세포에서 분비되며, 전두엽성 치매 (FTD)의 발병과의 관계가 주로 보고되었으나, MS 및 EAE에서는 PGRN의 기능 및 질병에 미치는 영향이 밝혀지지 않았다. 따라서 본 연구에서는 EAE 모델에서 PGRN의 발현과 질병의 진행간의 연관성을 평가하고, 이와 더불어

어 PGRN의 결핍이 EAE의 발병에 어떠한 영향을 미치는지 확인하고자 하였다. 우선 PGRN의 발현이 EAE의 임상증상이 심화될 수록 증가하는 것을 확인할 수 있었으며, 이러한 PGRN의 발현은 주로 정상세포, 미세아교세포, 중추신경계로 침윤된 염증세포에서 나타남을 확인할 수 있었다. 또한, PGRN 결핍 마우스에 EAE를 유발할 경우, 임상 증상 및 중추신경계의 염증의 유의적 감소가 확인되었으며, 말초의 자가항원 반응성 T 세포의 수적 감소가 나타남을 확인하였다. 결론적으로, 본 연구에서는 PGRN의 과발현은 EAE의 질병 유발에 영향을 미치는 것을 밝힘에 따라 PGRN을 MS의 새로운 치료 타겟으로 제시할 수 있을 것으로 사료된다.

주요어: 실험적 자가면역성 뇌척수염 (EAE); Progranulin; 다발성 경화증 (MS)